Observation of a transverse Meissner effect in Cu_{x}TiSe_{2} single crystals

Z. Medvecká, T. Klein, V. Cambel, J. Šoltýs, G. Karapetrov, F. Levy-Bertrand, B. Michon, C. Marcenat, Z. Pribulová, and P. Samuely

Phys. Rev. B **93**, 100501 — Published 7 March 2016

DOI: 10.1103/PhysRevB.93.100501

Observation of a transverse Meissner effect in Cu_xTiSe_2 single crystals

Z. Medvecká[1,2,3], T. Klein[1,2], V. Cambel[4], J. Šoltýs[4], G. Karapetrov[5], F. Levy-Bertrand[1,2], B. Michon[1,2], C. Marcenat[6,7], Z. Pribulová[3] and P. Samuely[3]

[1] *Université Grenoble Alpes, Inst NEEL, F-38042 Grenoble, France*

[2] *CNRS, Inst NEEL, F-38042 Grenoble, France*

[3] *Centre of Low Temperature Physics, IEP SAS and P.J.Safarik University, Park Angelinum 9, 04154 Kosice, Slovakia*

[4] *Institute of Electrical Engineering SAS, Dubravska cesta 9, 84104 Bratislava, Slovakia*

[5] *Department of Physics, Drexel University, 3141 Chestnut St., Philadelphia, PA 19104, USA*

[6] *Université Grenoble Alpes, INAC-SPSMS, F-38000, France and*

[7] *CEA, INAC-SPSMS, F-38000, France*

(Dated: February 16, 2016)

We report on local magnetization measurements showing the presence of an unexpectedly strong transverse Meissner effect in the superconducting Cu_xTiSe_2 single crystals. We show that for tilted magnetic fields (H_a) vortices remain aligned with the *ab*-planes up to field $H_k \sim H_p/\sin\theta_H$ (where θ_H is the angle between the applied field and the *ab*-plane and H_p the first penetration field) and that for $H_a > H_k$, the field dependence of the vortex direction $\theta_B(H_a)$ can be well described assuming that vortices remain partially locked in the planes forming a staircase structure of average direction $\theta_B \neq \theta_H$. This results indicate the existence of a strong modulation of the vortex core energy along the *c*-axis but its origin remains unclear.

Layered type-II superconductors has attracted considerable attention over the past decades since their anisotropic structure gives rise to a large variety of novel vortex phases (for a review see[1]). Indeed, the structure of the vortex matter is determined by the minimum of the total Gibbs energy which is sensitive to various microscopic parameters such as the mass anisotropy $\Gamma = \sqrt{m_c/m_{ab}}$, the Ginzburg-Landau parameter $\kappa = \lambda_{ab}/\xi_{ab}$ (λ_{ab} and ξ_{ab} being the in-plane London penetration depth and coherence length, respectively) and/or the nature of the defects present in the sample. In the case of large Γ (> 7) and κ (> 10) values, the angular dependence of the Gibbs energy[2] has for instance two degenerated minima and two distinct crossed vortex lattices can then coexist in the sample at the same time[3,4]. Furthermore, when ξ_c becomes on the order of the interlayer distance d, the modulation of the superconducting order parameter from plane to plane leads to the existence of a lock-in phase for which vortices penetrate into the sample with their normal cores locked between the layers[5,6] up to a field $H_L \sim [H_p/\sin\theta_H] \times [d/\xi_c]$ (where θ_H is the angle between the applied field and the plane and H_p the first penetration field at angle θ_H). Experimental evidence for this *intrinsic* lock-in effect have been obtained in both high T_c cuprates[7] and organic materials[8].

On the other hand, vortices can also be trapped by correlated pinning sites such as columnar defects[9] or twin planes[10] giving rise to an *extrinsic* lock-in effect (so-called *transverse* Meissner effect). This effect can then be observed for field orientations close to the correlated defects and the magnetic induction perpendicular to the defects remains null up to $H_L \sim [H_p/\sin\theta_H] \times \sqrt{\varepsilon_P/\varepsilon_l}$[11] where θ_H is now the angle between the magnetic field and the defect orientation, ε_l the line tension and ε_P the amount of core energy suppressed by the artificial structure. Note that in both intrinsic and extrinsic case, H_L scales as $1/\sin\theta_H$ and such a scaling is hence a strong signature for the existence of a lock-in effect. Finally note that, in the Bean model, the *irreversible* magnetic moment can also remain locked along the normal direction of thin plates up to a "critical" angle $\theta_c \approx arctan(w/l)$ due to geometrical effects[12] where w and l are the width and thickness of the slab, respectively.

We present here a detailed study of the field distribution in Cu doped $TiSe_2$[13] single crystals. The main result of our study is the clear evidence of an unexpected and large transverse Meissner effect for fields oriented close to the *ab*-planes. We show that vortices remain trapped along the layers up to an applied field $H_k(\theta_H) \sim H_p/\sin\theta_H$ (θ_H being the angle between the field and the plane) which can be attributed neither to the *intrinsic* lock-in effect as $\xi_c \approx 20$ nm[14] is much larger than $d \approx 0.6$ nm, nor to the existence of crossed lattices as the anisotropy is too small ($\Gamma \sim 1.7$). Our study hence strongly indicates the presence of correlated "defects" parallel to the *ab*-planes leading to a strong modulation of the vortex core energy along the *c*-direction. The nature of those "defects" still has to be clarified.

Cu_xTiSe_2 belongs to the group of transition metal dichalcogenides and shares some similarities with other unconventional materials such as their layered structure and the presence of an electronic instability competing with the superconducting state. Indeed, $TiSe_2$ hosts an excitonic charge density wave[15] which is progressively destroyed by copper intercalation between the $TiSe_2$ layers[13] giving rise to a superconducting dome in the phase diagram emerging above a doping content $x \sim 0.04$ with a maximum critical temperature $T_c \sim 4.1$ K reached around $x \sim 0.08$ where the quantum critical point is supposed to be. Three single crystals with different dopings from the underdoped, optimally doped to (slightly) overdoped regions of the phase diagram ($T_c = 2.8$ K, 4.1 K and 3.8 K i.e. $x \sim 0.06$, 0.08 and 0.085 for sample 1, 2 and 3 respectively) have been investigated. The re-

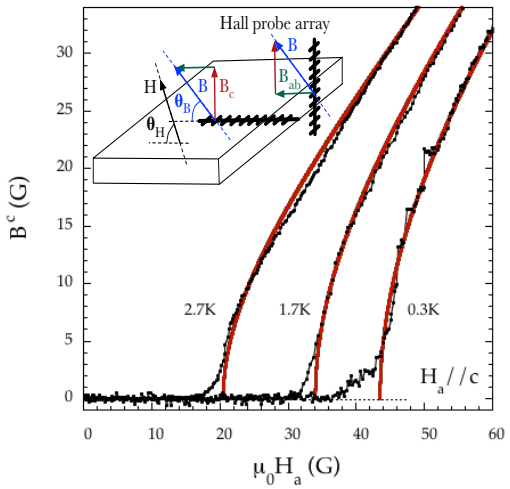

FIG. 1. (color online) Field dependence of the magnetic induction B^c for $H_a \| c$ in a Cu_xTiSe_2 single crystal at the indicated temperatures (sample 3). Solid (red) lines are fits to the data in the presence of geometrical barriers (see[20] and text for details). A small upturn in $B(H_a)$ visible close to H_p (corresponding to 5-10 vortices) can be attributed to the presence of low but non-zero bulk pinning. Inset: Scheme of the experimental setup to measure different components of B by Hall probes.

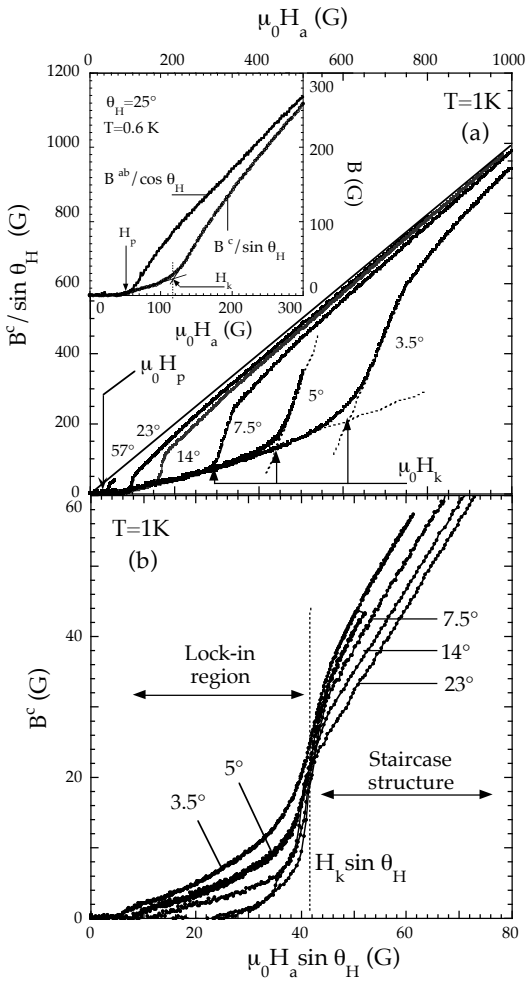

FIG. 2. Upper panel (a) : magnetic field dependence of $B^c/\sin\theta_H = B \times [\sin\theta_B/\sin\theta_H]$ in Cu_xTiSe_2 (sample 3) for the indicated field orientations θ_H (θ_B being the orientation of the induction inside of the sample, see text for details). As shown for large θ_H values, B^c rapidly increases for $H_a > H_p$ (see also Fig.1 for $\theta_H = 90°$), whereas for smaller θ_H values, B^c remains small ($\theta_B \approx 0$) up to H_k which clearly indicating the presence of a transverse Meissner effect. The non-zero B^c value (for $H_p < H_a < H_k$) probably originates in the small but non-zero distance between the probe and the sample surface. As shown, B^c (and hence θ_B) rapidly increases for $H_a > H_k$ indicating a rapid change in the orientation of the flux lines. Inset : Magnetic field dependence of the $B^c/\sin\theta_H$ and $B^{ab}/\cos\theta_H$ components of the induction for $\theta_H = 25°$ at $T = 0.6$ K (sample 2). Lower panel (b) : curves from Fig.2a scaled by $\sin\theta_H$ showing that $H_k \sin\theta_H \sim 40$ G (at 1 K), being close to the H_p^c value of the sample (see also Fig.3).

sponse of the samples to an applied magnetic field has been measured by an array of 10 miniature GaAs-based quantum well Hall sensors with dimensions 10x10 μm^2 and a pitch of 30 μm. The sample (of typical dimensions $\sim 500 \times 500 \times 100$ μm^3) was placed on the top of the probes and cooled down in zero magnetic field to the lowest temperature of 0.3 K. The Hall voltage has been converted into local magnetic induction B using the respective probe sensitivity. The field dependence for both components of the induction, $B^c = B\sin\theta_B$ and $B^{ab} = B\cos\theta_B$, were obtained by placing the probes either perpendicularly or parallel to the sample ab-planes (see sketch in the inset of Fig.1) for a given temperature and θ_H value. The B^c/B^{ab} ratio between those two components then led to the field dependence of the *vortex* orientation $\theta_B(H_a)$. As discussed below for applied field oriented close to ab-planes, θ_B clearly differs from θ_H for low magnetic fields but tends towards θ_H with increasing fields.

The main panel of Fig.1 displays the field dependence of B^c for increasing H_a oriented parallel to the $c-$axis ($\theta_H = 90°$). For small magnetic field B^c remains zero as the sample screens out the field from the Hall sensors in the Meissner state. When H_a reaches the first penetration field H_p, vortices start to penetrate into the sample and the signal becomes non zero. This sharp increase in B^c (common to all three samples) clearly indicates that pinning by point defects is extremely small in this system[16,17]. As shown in Fig.1 (solid red lines), $B^c(H_a)$ can be well described by a $\mu_0 H_a\sqrt{1-(H_p/H_a)^2}$ law as proposed by Zeldov *et al.*[18] in the case of a penetration process dominated by geometrical barriers[19,20]. The small upturn in the signal visible close to H_p (corresponding to 5-10 vortices) indicates the presence of very low[17] but non-zero bulk (point) pinning which does not change the conclusions drawn below. The main influ-

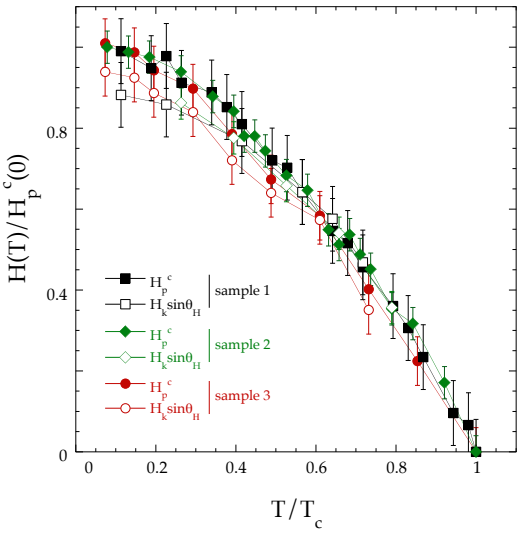

FIG. 3. (color online) Temperature dependence of the first penetration field H_p^c (solid symbols) for $H_a \| c$ in sample 1 (black squares), 2 ((green) diamonds) and 3 (red circles) for $H_a || c$ (see Fig.1) and $H_k \sin\theta_H$ (open symbols) where H_k is the lock-in field observed for tilted magnetic fields (see Fig.2 and text for details). As shown, in all samples, $H_k \sin\theta_H \sim H_p$, traking its temperature dependence on a large part of the diagram.

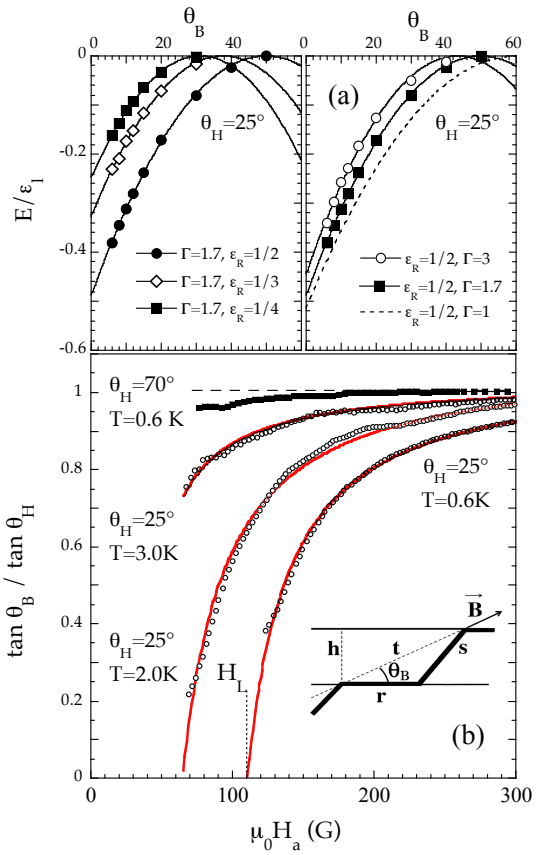

FIG. 4. (color online) Upper panel (a) : angular dependence of the pinning energy for the staircase vortex structure sketched in the inset of Fig.4b and for the indicated $\varepsilon_R = \Gamma\varepsilon_P/\varepsilon_l$ and Γ values (see text for details). The dotted line (right panel) corresponds to the analytical dependence obtained in the isotropic case ($\Gamma = 1$) and the solid lines are parabolic fits to the data (see text for details). Lower panel (b) : field dependence of the orientation of the induction (θ_B) for $\theta_H = 25°$ (open circles) and $\theta_H = 70°$ (closed squares) at the indicated T values. Data for $\theta_H = 25°$ and $T = 0.6$K has been deduced from the measurements displayed in the inset of Fig.2a. The solid (red) lines are fits to the data using Eq.(2). As shown, for $\theta_H = 25°$, a very reasonable agreement is obtained up to 3.0 K ($0.7T_c$) whereas for large θ_H values ($\theta_H > \theta_t$), $\theta_B \approx \theta_H$ even at low temperature.

ence of the geometrical barriers is further confirmed by the dome-like shape of the field profiles reported in[16] for $H_a > H_p$, clearly showing that the vortices first accumulate in the center of the sample. H_p was thus detected by probes located close to the center of the sample but for the discussion below it is important to note that geometrical barriers do not play any role for fields exceeding $\sim 2H_p$[18,21] and the lockin effect discussed below can not be related to the field penetration process.

The $B^c(H_a)$ dependence measured for various field orientations θ_H is displayed in Fig.2a. As discussed above, for large field angles θ_H, B^c sharply increases when vortices penetrate into the sample at $H_a = H_p$. On the other hand, for fields oriented close to the ab-plane, a second characteristic field can be clearly recognized in the $B^c(H_a)$ curves. As shown for $\theta_H < 23°$, B^c remains close to zero well above the first penetration field and a sharp kink appears in B^c when H_a reaches a characteristic field, called here H_k. The reduced B^c value observed for $H_p < H_a < H_k$ is strongly suggesting that vortices penetrating into the sample remain trapped along the ab-planes and leave the sample through the sides perpendicular to the ab-planes, being hence not detected by the Hall probes. The non zero B^c signal in this field range probably originates from the small but non zero distance between the probe and the sample surface. When $H_a = H_k$, vortices unlock and the rapid change in their orientation leads to the sharp increase in B^c (see discussion below). Note that the angular dependence of H_p depends on the geometrical factors and the mass anisotropy with $H_p^{ab}/H_p^c \sim (\sqrt{w/l}).(H_{c1}^{ab}/H_{c1}^c) \sim \sqrt{w/l\Gamma^2}$[18,21]. For sample 2, $H_p^{ab}/H_p^c \sim 1$ (geometrical factors compensating the anisotropy) rising up $\sim$ 2 in sample 1 and 3. However, since H_k largely exceeds this value for small angles, the observed increase in B_c at H_k can not be mistaken for vortex penetration.

Fig.2b displays the curves from Fig.2a plotted as a function of $H_a \sin\theta_H$. As clearly shown, all the upturns in B^c at $H_k \sin\theta_H$ collapse onto the same value as expected for the lock-in effect. Note that the "critical" lock-in angle scales as $\sin\theta_H \propto 1/H_a$ and can hence not be attributed to geometrical effects[12]. Moreover

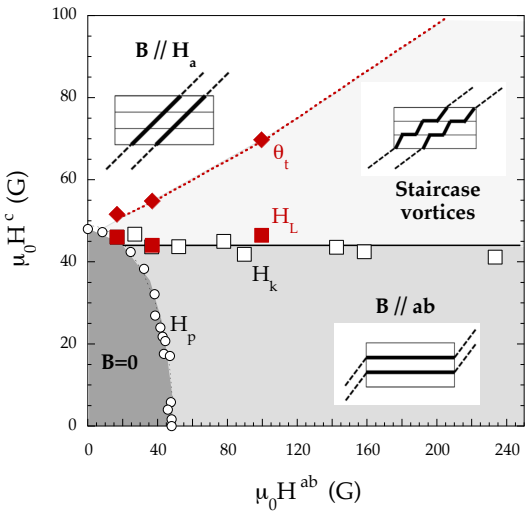

FIG. 5. (color online) Phase diagram of the vortex structure in Cu_xTiSe_2 as a function of the field orientation (sample 2). H_k and H_p values have been obtained directly from the $B^c(H_a)$ curves for various field orientation (see Fig.4*a* for $\theta_H = 25°$) while H_L and θ_t are the parameters deduced from the fits to the data using Eq.(2) (solid red lines in Fig.4*b*). Similar phase diagrams were obtained for all 3 studied samples with different copper concentration.

$H_k \sin\theta_H \sim H_p^c$ emphasizing that the lock-in field is close to its maximum value and the lock-in effect is particularly strong in our system. This scaling has been observed in all measured samples (i.e. whatever the doping content) and at temperatures up to $T/T_c \sim 0.7 - 0.8$ (see Fig.3). For higher temperatures H_k could not be distinguished from H_p anymore.

To analyse the field dependence of the vortex orientation into more details both B^c and B^{ab} components of the magnetic induction were needed. The inset of Fig.2a displays the field dependence of $B^{ab}/\cos\theta_H = B[\cos\theta_B/\cos\theta_H]$ and $B^c/\sin\theta_H = B[\sin\theta_B/\sin\theta_H]$ for $\theta_H = 25°$. If vortices were aligned with the magnetic field ($\theta_H = \theta_B$) the two signals would be equal (to B) which is obviously not the case. Indeed, in contrast to the rapid increase in $B^{ab}/\cos\theta_H$ for$H_a > H_p$, the field detected perpendicular to the planes $B^c/\sin\theta_H$ remains small up to H_k. This clearly shows that for $H_a > H_p$ vortices present in the sample do not intersect the *ab*-plane and remain locked in this plane up to H_k. The field dependence of the vortex orientation ($\tan\theta_B/\tan\theta_H$) for $H_a > H_k$ is obtained by dividing the two components of the magnetic induction and is displayed in Fig.4b.

To theoretically describe this field dependence, we started with the standard London model. In the absence of disorder, the vortex structure results from the minimization of the total Gibbs energy density[2]:

$$G = \frac{B^2}{2\mu_0} + \frac{\varepsilon_l B}{\Phi_0} f(\theta_B, \Gamma, \kappa) - BHcos(\theta_B - \theta_H) \qquad (1)$$

for $H \sim H_{c1}$ ($H_a \sim H_p$), where Γ is the anisotropy, κ the Ginzburg-Landau parameter, ε_l the line tension : $\Phi_0^2 \ln\kappa/4\pi\mu_0\lambda_{ab}^2$ and $f(\theta, \Gamma, \kappa)$ the angular dependence of the core energy[2]. Given the reduced κ and Γ values of our system, the observed lockin effect can not be related to the possible coexistence of crossed lattices[2] and it is hence necessary to add some extra (pinning) contribution to the Gibbs energy in order to account for the observed behavior. As suggested by Blatter *et al.*[11] the formation of a staircase structure in presence of correlated defects can be described by assuming that this pinning energy can be written as: $\mathcal{E}(\theta_B, r(\theta'_B)) = r(\varepsilon_l/\Gamma - \varepsilon_P) + s\varepsilon_l f(\theta'_B) - t\varepsilon_l f(\theta_B)$ (see sketch in the inset of Fig.4b for the definition of r, s and t). The "optimal" energy gain ($\mathcal{E}_{opt}(\theta_B, r_{opt})$) is then obtained by minimizing $\mathcal{E}$ with respect to r and the corresponding energy density $E = B\mathcal{E}_{opt}/\Phi_0 t$ is obtained by accounting for a small but finite density of vortices equal to $1/a_0^2 t$ (with $a_0^2 = \Phi_0/B$).

We have extended the model discussed in[11] in order to include the anisotropy factor Γ and large θ_B values. Numerical solutions for selected Γ and $\varepsilon_R = \Gamma\varepsilon_P/\varepsilon_l$ values are displayed in of Fig.4a together with the analytical solution obtained for isotropic systems (dotted line) for which $E(\theta_B) = \varepsilon_l(B/\phi_0)[(1-\varepsilon_R)\cos\theta_B + \sqrt{2\varepsilon_R - \varepsilon_R^2}\sin\theta_B - 1]$. As shown, E can be very well described by a simple parabolic approximation for all investigated ε_R and Γ values (solid lines) : $E(\theta_B, \Gamma, \varepsilon_R) \approx -\frac{1}{2}\tilde{\varepsilon_l}(\Gamma, \varepsilon_R)(\theta_B - \theta_t(\Gamma, \varepsilon_R))^2$ hence generalizing the result previously obtained for small angles in[11]. As shown, $\tilde{\varepsilon_l}$ is almost independent of ε_R (increasing slightly with Γ) whereas the critical trapping angle θ_t increases for increasing ε_R values (with $\tan\theta_t = \sqrt{2\varepsilon_R - \varepsilon_R^2}/(1-\varepsilon_R)$ in the isotropic case). In this parabolic approximation, the minimization of the total Gibbs energy density with respect to θ_B then leads to :

$$\frac{\tan\theta_B}{\tan\theta_H} \approx \begin{cases} 0 & H < H_L \\ \dfrac{1 - \frac{H_L}{H}}{1 - \frac{H_L}{H}\frac{\tan\theta_H}{\tan\theta_t}} & H_L < H, \theta_H < \theta_t \\ 1 & \theta_t < \theta_H \end{cases} \qquad (2)$$

where the lock-in field $H_L \approx [H_{c1}^c/\sin\theta_H]\mathcal{F}(\Gamma, \varepsilon_R)$ (with $\mathcal{F} = (2\varepsilon_R - \varepsilon_R^2)^{1/2}$ for $\Gamma = 1$). This equation describes three phases of vortex structure: at first the lock-in effect ($\theta_B = 0$) for $H < H_L$, then the staircase structure for $H > H_L$ and finally $\theta_B = \theta_H$ when vortices align with the applied field.

As shown in Fig.4b (solid red lines), very reasonable fits to the data can be obtained using Eq.(2) supporting the existence of a staircase structure for $H_a > H_k$, on a large temperature range (see also Fig.3). As expected, the H_L values deduced from Eq.(2) are indeed equal to the H_k values directly deduced from the sharp increase in B^c observed in Fig.2a. Note that since $\Gamma = 1.7$, the small but non zero angular dependence of the second term in Eq.(1) has been neglected. However we have numerically checked that this angular dependence only induces small shifts in the θ_B values (typically by 1°-2°). Similarly, we

did not take into account the field dependence of the demagnetization effect simply assuming that the real magnetic field $H = \alpha(\theta_H)H_a$ but again, this only induces minor quantitative changes in the fitting parameters as α is close to 1 for $\theta_H = 25°$.

In summary, Fig.5 displays the vortex phase diagram of Cu_xTiSe_2 crystals deduced from our vectoriel magnetization measurements. Very similar phase diagrams were obtained for all three samples. We have shown that vortices remain locked along the *ab*-planes, up to a lock-in field H_L. For $H_a > H_L$ the field dependance of the orientation of the vortices can be well described assuming that the vortex matter forms a staircase structure. $H_L = [H_p^c/\sin\theta_H] \times \mathcal{F}(\Gamma, \varepsilon_R) \approx H_p^c/\sin\theta_H$ indicating that the suppression of the core energy is very strong ($\varepsilon_R \sim 1$), largely exceeding the value expected for twin planes ($\varepsilon_R \sim 10^{-3}$)[11]. It has been suggested[22] that spatial modulations of the superconducting order parameter could exist in systems with competing - and coupled - order parameters in presence of defects which could locally alter the competing phase but, as the effect has been observed in all three samples (from underdoped to slightly overdoped), it can not be directly related to the charge properties of the system. The nature of the "defects" leading to such a strong modulation of the core energy hence still has to be be clarified.

This work is supported by the French National Research Agency through Grant No. ANR-12-JS04-0003-01 SUBRISSYME. Z.M thanks Campus France for financial support (Eiffel PhD grant). The work at Drexel is supported by the National Science Foundation under Grant No. ECCS-1408151, the Slovak Research and Development Agency Contracts No. APVV-0036-11, APVV-14-0605, VEGA No. 2/0135/13 and the international project COST Action MP 1201.

[1] G. Blatter, M. Y. Feigel'man, Y. B. Geshkenbein, A. I. Larkin, V. M. Vinokur, Rev. of Mod. Phys. **66**, 1321 (1994).
[2] A. Sudbø, E. H. Brandt and D. A. Huse, Phys.Rev. Lett. **71**, 1451 (1993).
[3] A. Grigorenko, S. Bending, T. Tamegai, S. Ooi and M.Henini, Nature **414**, 728 (2001).
[4] V. O. Dolocan, P. Lejay, D. Mailly, and K. Hasselbach, Phys. Rev. B **74**, 144505 (2006).
[5] L.N.Bulaevskii, Phys. Rev. B **44**, 910(R) (1991).
[6] D. Feinberg and A. M. Ettouhami, Int. J. of Mod. Phys. B7, 2085-2108 (1993)
[7] M. Tachiki and S. Takahashi, Solid State Commun. **70**, 291 (1989); D. E. Farrell, J. P. Rice, D. M. Ginsberg, and J. Z. Liu, Phys. Rev. Lett. **64**, 1573 (1990); W. K. Kwok, U. Welp, V. M. Vinokur, S. Fleshier, J. Downey, and G. W. Crabtree, Phys. Rev. Lett. **67**, 390 (1991); Yu. V. Bugoslavsky, A. A. Zhukov, G. K. Perkins, A. D. Caplin, H. Kojima and I. Tanaka, Phys. Rev. B, **56**, 5610 (1997).
[8] P.A. Mansky, P M. Chaikin and R.C. Haddon, Phys. Rev. Lett. **70**, 1323 (1993).
[9] A. Silhanek, L. Civale, S. Candia, G. Nieva, G. Pasquini and H. Lanza, Phys. Rev. B **59**, 13620 (1999); T. Klein, A. Conde-Gallardo, I. Joumard, and J. Marcus, C. J. van der Beek and M. Konczykowski, Phys. Rev. B **61**, R3830 (2000).
[10] M. Oussena, P. A. J. de Groot, K. Deligiannis, A. V. Volkozub, R. Gagnon, and L. Taillefer, Phys. Rev. Lett. **76**, 2559 (1996); B. Keimer, F. Dogan, A. Aksay, R.W. Erwin, J.W. Lynn and M. Sarikaya, Science **262**, 83 (1993).
[11] G. Blatter, J. Rhyner and V. M. Vinokur, Phys. Rev. B, **43**, 7826 (1991); A. A. Zhukov, G. K. Perkins, J. V. Thomas, A. D. Caplin, H. Kpfer, and T. Wolf, Phys. Rev. B, **56**, 3481 (1997).
[12] A. A. Zhukov, G. K. Perkins, Yu. V. Bugoslavsky, and A. D. Caplin, Phys. Rev. B, **56**, 2809 (1997).
[13] E. Morosan, H.W. Zandbergen, B.S. Dennis, J.W.G. Bos, Y. Onose, T. Klimczuk, A.P. Ramirez, N.P. Ong and J. Cava, Nature Physics, **2**, 544 (2006).
[14] J. Kačmarčík, Z. Pribulová, V. Paľuchová, P. Szabó, P. Husaníková, G. Karapetrov and P. Samuely, Phys. Rev. B, **88**, 020507(R) (2013).
[15] H. Cercellier, C. Monney, F. Clerc, C. Battaglia, L. Despont, M. G. Garnier, H. Beck, P. Aebi, L. Patthey, H. Berger, and L. Forro, Phys. Rev. Lett., **99**, 146403 (2007).
[16] Z. Pribulová, Z. Medvecká, J. Kačmarčík, V. Komanický, T. Klein, P. Husaníková, V. Cambel, J. Šoltýs, G. Karapetrov, P. Samuely, Acta Physica Polonica A, **126**, 370 (2014).
[17] The critical current deduced from the value of the remanent induction is only on the order of a few 10^{-4}A/cm^2 (at 0.3 K and $H\|c$) being similar to the value obtained in high quality MgB_2 single crystals (see [20]) and being several orders of magnitude smaller than in pnictides, see for instance : C. J. van der Beek, G. Rizza, M. Konczykowski, P. Fertey, I. Monnet, Thierry Klein, R. Okazaki, M. Ishikado, H. Kito, A. Iyo, H. Eisaki, S. Shamoto, M. E. Tillman, S. L. Budko, P. C. Canfield, T. Shibauchi, and Y. Matsuda, Phys. Rev. B **81**, 174517 (2010).
[18] E. Zeldov, A. I. Larkin, V. B. Geshkenbein, M. Konczykowski, D. Majer, B. Khaykovich, V. M. Vinokur, and H. Shtrikman, Phys. Rev. Lett. **73**, 1428 (1994).
[19] L. Lyard, T. Klein, J. Marcus, R. Brusetti, C. Marcenat, M. Konczykowski, V. Mosser, K. H. Kim, B. W. Kang, H. S. Lee, and S. I. Lee, Phys. Rev. B **70**, 180504(R) (2004).
[20] E. Zeldov, D. Majer, M. Konczykowski, A. I. Larkin, V. M. Vinokur, V. B. Geshkenbein, N. Chikumoto, and H. Shtrikman, Europhys. Lett. **30**, 367 (1995).
[21] E.H. Brandt Phys. Rev. B **59**, 3369 (1999).
[22] A. Moor, A.F. Volkov, and K.B. Efetov, Phys. Rev. B, **91**, 064511(2015).